THE JOURNAL OF PHYSICAL CHEMISTRY B

Article

pubs.acs.org/JPCB

Length Scales and Structural Dynamics in Nematogen Pseudonematic Domains Measured with 2D IR Vibrational Echoes and Optical Kerr Effect Experiments

Kathleen P. Sokolowsky, Heather E. Bailey, and Michael D. Fayer*

Department of Chemistry, Stanford University, Stanford, California 94305, United States

ABSTRACT: Nematogen liquids in the isotropic phase are macroscopically homogeneous but on multinanometer length scales have pseudonematic domains with correlation lengths that grow as the isotropic to nematic phase transition temperature (T_{NI}) is approached from above. Orientational relaxation of nematogens in the isotropic phase manifests as two fast power laws and a slow exponential decay when measured by optical heterodyne detected optical Kerr effect (OHD-OKE) experiments. The long time exponential relaxation is associated with complete randomization of pseudonematic domains. We examine the effect of local orientational correlation on spectral diffusion (structural evolution) experienced by a vibrational probe molecule within the pseudonematic domains of 4-cyano-4′-pentylbiphenyl (5CB) using two-dimensional infrared (2D IR) vibrational echo spectroscopy. The addition of low concentration 4-pentyl-4′-thiocyanobiphenyl (5SCB) as a long-lived vibrational probe to 5CB is shown to lower T_{NI} of the sample slightly, but the fast power law dynamics and exponential decays observed by OHD-OKE spectroscopy are unchanged. We compare the complete orientational relaxation and spectral diffusion for samples of 5SCB in 5CB to 5SCB in 4-pentylbiphenyl (5B) at four temperatures above T_{NI}. 5B has a molecular structure similar to 5CB but is not a nematogen. At all but the lowest temperature, the spectral diffusion in 5CB and 5B is described well as a triexponential decay with very similar time constants. The results demonstrate that the presence of local orientational order at temperatures well above T_{NI} does not affect the spectral diffusion (structural evolution) within pseudonematic domains when the correlation lengths are short. However, when the temperature of the sample is held very close to T_{NI}, the spectral diffusion in 5CB slows dramatically while that in 5B does not. It is only as the correlation length becomes very long that its presence impacts the spectral diffusion (structural fluctuations) sensed by the vibrational probes located in pseudonematic domains. The orientational relaxation is modeled with schematic mode coupling theory (MCT). Fitting with MCT provides density and orientational correlation functions. The density correlation decays are similar for 5B and 5CB, but the orientational correlation decays are much slower for 5CB. Additionally, the time dependence of the spectral diffusion in 5CB is strikingly similar to that of the density correlation function decay, while the orientational correlation function decay is far too slow to contribute to the spectral diffusion. Therefore, density fluctuations are likely the source of spectral diffusion at temperatures at least 5 K above T_{NI}.

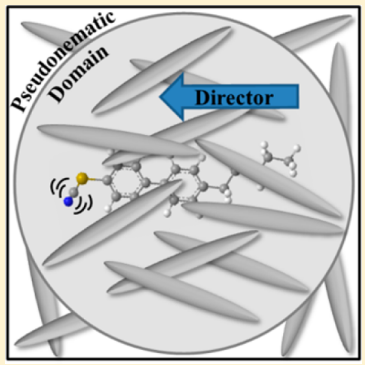

I. INTRODUCTION

Nematogens in the isotropic phase display dramatically different temperature dependent orientational relaxation dynamics compared to normal liquids. At temperatures above the nematic−isotropic phase transition temperature, T_{NI}, these dynamics are heavily influenced by the presence of pseudonematic domains characterized by correlation length ξ.[1] The temperature (T) dependence of the correlation length is described by Landau−de Gennes theory.[1] $\xi(T)$ is given by

$$\xi(T) = \xi_0[T^*/(T - T^*)]^{1/2}, \quad T > T^* \tag{1}$$

where ξ_0 is the molecular length scale (4−5 Å)[2−4] and T^* is a temperature slightly below (typically 0.5−1 K) T_{NI}. The final slow exponential decay observed in orientational relaxation is related to the complete randomization of pseudonematic domains.[5−9] The relaxation time, τ_{LdG}, of this decay increases and then diverges as T^* is approached from above[6,10,11] due to the growing correlation length.[1]

$$\tau_{LdG} = \frac{V^*_{eff}\eta(T)}{k_B(T - T^*)} \tag{2}$$

where $\eta(T)$ is the viscosity, V^*_{eff} is the effective volume, and k_B is the Boltzmann constant.

The existence of pseudonematic domains offers a unique opportunity to study the influence of nanoscopic length scales on dynamics in a single component system. There are many examples in which the molecules of a liquid in systems limited to a length scale of a few nanometers have dynamics that are fundamentally different from those in the corresponding bulk liquid. For example, water in reverse micelles has dynamics that differ greatly from bulk water.[12] However, the change in water

Special Issue: James L. Skinner Festschrift

Received: January 6, 2014
Revised: February 8, 2014
Published: February 12, 2014

dynamics is caused by the presence of the interface between water and the surfactant that comprises the reverse micelles. For sufficiently large reverse micelles, water has bulk dynamics in the central core of the water pool, while it has substantially slower dynamics at the interface.[12,13] Benzene in nanoporous sol−gel glass monoliths displays orientational dynamics distinct from bulk benzene because of interactions with the interfaces.[14] Water in the nanochannels of Nafion fuel cell membranes and water between the planar layers of lamellae display dynamics that differ from the bulk because of the presence of an interface.[15,16] The deviations in these and many other systems are induced by the presence of another species. Interactions with another species, an interface, or, as another example, charged regions of a room temperature ionic liquid[17,18] often induce a degree of ordering in the liquid under study. Nematogens in the isotropic phase are novel in that the long-range ordering is an inherent property of the molecules. The polar and rod-shaped nature of many nematogens (alkyl-cyanobiphenyls, benzophenone, phenyl salicylate, etc.)[10,11] induces the self-ordering seen in these systems. Additionally, control over the size (correlation length) of the ordered regions is made possible by controlling the temperature of the sample.

In this paper, we begin to elucidate the effect of pseudonematic domains on nematogen molecules' dynamics through temperature dependent ultrafast two-dimensional infrared (2D IR) vibrational echo experiments, other ultrafast IR experiments, and optical heterodyne detected optical Kerr effect (OHD-OKE) experiments. The 2D IR experiments yield information on the dynamics experienced by molecules in the pseudonematic domains, while the OHD-OKE experiments provide dynamical information on the bulk nematogen liquid. For comparison, the experiments are conducted on a molecule that is not a nematogen but has a structure very similar to the nematogen.

The requirement of a vibrational probe in 2D IR studies influenced the choice of 4-cyano-4′-pentylbiphenyl (5CB) as the liquid crystal for study. The nematic−isotropic phase transition temperature of 5CB is 35 °C.[19] In the present study, 5CB in the isotropic phase was examined up to 40 °C above the transition temperature. The nitrile stretch of 5CB is a sharp peak at 2230 cm^{-1}.[20] Previous work has shown that using the CN stretch of 5CB as a vibrational probe resulted in significant experimental problems.[21] The lifetime of the CN stretch is short, ∼4 ps, and because the sample is a pure liquid, it needed to be exceedingly thin, a few micrometers, to keep the absorbance sufficiently low to perform the experiments. Vibrational relaxation produced excessive heating that generated additional thermally induced peaks in the 2D IR spectrum.[21] The heat deposition limited the measurements to 6 ps. The heating problem was circumvented by using the natural abundance ^{13}CN peak as the probe. Because carbon-13 is ∼1% natural abundance, the absorbance was greatly reduced, and a thicker sample could be used, which eliminated the heating problem. In addition, the ^{13}CN stretch of 5CB (5^{13}CB) has a vibrational lifetime of ∼8 ps, making it possible to perform the 2D IR measurements to ∼25 ps.[21] To further increase the 2D IR experimental time window in 5CB, a small amount of the dopant molecule 4-pentyl-4′-thiocyanobiphenyl (5SCB) was added. While 5SCB is structurally similar to 5CB, the addition of a heavy "blocking" atom increased the lifetime of the nitrile vibrational stretch to ∼100 ps, making it possible to observe the dynamics with 2D IR to ∼200 ps.[21] The 2D IR measurements on 5SCB in 5CB were compared to those made on 5CB and 5^{13}CB. The decays are identical within experimental error over the time ranges in which the data from the three samples could be compared.[21] Therefore, 5SCB can be used as the vibrational probe. 5SCB provides a lifetime that is sufficiently long to observe the complete 2D IR measured dynamics at all but the lowest temperature.

Previous OHD-OKE experiments on nematogens show the existence of fast, nonexponential decays prior to the final exponential decay. These fast decays are not described by Landau−de Gennes theory.[6,10,11,22,23] The OHD-OKE experiment measures the time derivative of the polarizability−polarizability correlation function, which is equivalent to the orientational correlation function except at very short times, less than a few picoseconds.[24,25] The data for nematogens in the isotropic phase can be fit with a phenomenological fitting function consisting of two power laws multiplied by the Landau−de Gennes exponential decay.[22,23,26] The form of this function is based on schematic mode coupling theory (MCT) and is useful to extract parameters, particularly τ_{LdG}.

OHD-OKE data can be analyzed in more detail using a modified version of MCT.[23] On the basis of the Sjögren model of schematic MCT, the nematogen isotropic phase MCT theory employs two correlation functions, the density correlation function and the orientational correlation function. The time derivative of the orientational correlation function is the measured OHD-OKE decay.[23,27,28] The orientational correlation function is coupled to the density correlation function. Both correlation functions can be extracted when the OHD-OKE data are fit. Modifications to the Sjögren model were implemented to account for the divergence of the final exponential decays as T^* is approached in the nematogen isotropic phase.[23]

While OHD-OKE experiments can be conducted over a wide range of time scales (∼100 fs to ∼1 μs), they measure the collective orientational relaxation dynamics. OHD-OKE experiments are unable to address the dynamics of the individual molecules within pseudonematic domains. To study the dynamics that arise from the full range of molecular motions, the 2D IR vibrational echo experiments are used to augment the OHD-OKE measurements. 2D IR spectroscopy provides information on structural dynamics through the measurement of spectral diffusion of a vibrational oscillator,[29−31] in this case the CN stretch of 5SCB in 5CB. The CN stretch absorption band is inhomogeneously broadened because of the variety of structural environments that exist at an instant of time. Spectral diffusion is the time evolution of the initial frequencies of the vibrations, which is caused by the structural fluctuations of the system. Combining the 2D IR spectral diffusion data with bulk orientational relaxation data from OHD-OKE provides a detailed picture of the structural evolution in 5CB.

OHD-OKE studies have previously been conducted on 5CB in the isotropic and nematic phases.[10,11,22,26,32] We present OHD-OKE data on a solution of 5CB doped with a small amount of 5SCB to test the effect of 5SCB on the bulk liquid properties. The decays observed for the doped sample are nearly identical to those of neat 5CB; the final exponential decay at a given temperature is slightly faster. The experiments show that T^* for the doped sample has been lowered by about 3 °C compared to the neat sample. Thus, the addition of 5SCB does not substantially perturb the nature of the liquid dynamics in 5CB but is slightly temperature shifting them. Thus, we can probe the structural dynamics of 5CB with the 5SCB

dx.doi.org/10.1021/jp500144p | J. Phys. Chem. B 2014, 118, 7856−7868

vibrational probe without significantly changing the liquid crystal system.

As a complement to experiments on the liquid crystal 5CB, the structurally similar 4-pentylbiphenyl (5B) was also studied. Other than lacking the nitrile group, 5B is molecularly identical to 5CB; however, 5B is not a nematogen.[33] The OHD-OKE decays obtained for 5B as a function of temperature have the same form as those of 5CB, two power laws and a final exponential decay, but the exponential decay is dramatically faster in 5B due to the lack of correlated pseudonematic domains. Additionally, schematic MCT analysis of both 5B and 5CB was performed to obtain density and orientational correlation functions. The density correlation decays obtained for 5B and 5CB are fairly similar. Orientational correlation functions found via schematic MCT fitting for the two compounds are dramatically different in time scale; the 5CB correlation decay is much slower.

2D IR experiments on 5SCB in both 5B and 5CB reveal very similar structural dynamics at temperatures at least 5 °C above T_{NI}. The spectral diffusion of the nitrile stretch of 5SCB presents as a triexponential decay with comparable time constants in both liquids. In 5CB, there is no evidence to suggest that the probe molecule is affected by the orientational correlation associated with a pseudonematic domain. Time constants of the spectral diffusion are remarkably similar to those obtained from the triexponential fit of the density correlation function from the schematic MCT analysis. The results suggest that density rather than orientational fluctuations are the cause of spectral diffusion in 5CB and 5B at temperatures significantly above T_{NI}. However, as T^* is approached, the 5CB and 5B dynamics differ substantially. At approximately 2 °C above T^*, the structural dynamics of 5CB slow significantly. The spectral diffusion observed in 5B is not equally affected at the same temperature. The divergence in behavior of the spectral diffusion in 5CB relative to 5B indicates that the correlation in pseudonematic domains influences the spectral diffusion only when the correlation length ξ becomes large at temperatures very close to T^*.

II. EXPERIMENTAL PROCEDURES

A. Sample Preparation. 5CB and 5B were purchased from Sigma-Aldrich and TCI America, respectively, and were used without further purification. 5SCB was synthesized as previously described.[21] Solutions of 5SCB in 5CB or 5B were prepared by dissolving approximately 2.5 mol % 5SCB in the host liquid. The resulting solutions were passed through a 0.1 μm filter (Anotop) before being loaded into the appropriate sample cell.

For OHD-OKE experiments, samples were contained between two 3 mm thick CaF_2 windows held at a 1 cm path length in a custom cell. For FT-IR and ultrafast infrared experiments, samples were sandwiched between two 3 mm thick CaF_2 windows, separated by a 250 μm Teflon spacer. The CaF_2 windows were held in a copper sample cell. In both experimental setups, the sample cell temperature was varied from approximately 305 to 350 K, maintained to ±0.1 K with a PID temperature controller. The viscosity of all solutions was measured as a function of temperature with a Brookfield DV-II + Pro viscometer with a small volume cone plate adapter.

B. Optical Heterodyne Detected-Optical Kerr Effect Spectroscopy. The OHD-OKE experiment is a nonresonant ultrafast spectroscopic technique in which a linearly polarized pump pulse induces a transient birefringence in an initially isotropic sample. The time decay of the birefringence, which is a measurement of orientational relaxation, is monitored via a time-delayed probe pulse linearly polarized at 45° relative to the pump. Optical heterodyne detection is achieved by making the probe polarization slightly elliptical, thereby introducing a collinear and in-phase local oscillator.[34,35]

The general details of the optical Kerr effect setup have been described previously[18] with modifications for probing into the microsecond regime made to improve the signal-to-noise ratio.[17] Briefly, a 5 kHz Ti:sapphire regenerative amplifier seeded by a mode-locked 86 MHz Ti:sapphire oscillator is used to generate laser pulses with widths varying from 60 fs to 125 ps and powers up to 300 μJ per pulse. The laser pulses are beam split into pump and probe pulses. The probe's ellipticity is modulated at 2.5 kHz with a Pockels cell. The pump polarization is modulated at 1.25 kHz with another Pockels cell, and the signal is detected at the 1.25 kHz frequency with a balanced detector and lock-in amplifier.

Because of the nonresonant nature of the experiment, the pulses can be chirped without interfering with the measured dynamics. For the shortest times, the pulses were ∼60 fs in duration. For the longer time scale portions of the decays, pulses of longer duration, which yield more signal, were produced by increasing the chirp. Scans taken with various pulse widths are then overlapped in software to produce the full OHD-OKE curve. To collect data past the 15 ns window of the long delay stage, continuous wave (CW) probing was implemented. A portion of the 532 nm CW oscillator pump laser is diffracted via an acousto-optic modulator to generate 2 μs pulses at 5 kHz. This CW probe is then crossed with the pump beam at the sample, and its transient response is recorded with a fast photomultiplier tube (Hamamatsu, R7400U) and fast digitizer (Agilent Acquiris DP110, 1 GS/s). For CW probing, the pump beam is a ∼13 ns pulse coming from the free lasing output of the unseeded regenerative amplifier. CW probing data were scaled, overlapped, and combined in software with the pulsed probing data to generate the full OHD-OKE decay curve.

OHD-OKE data were collected for the four samples (both neat and doped 5CB and 5B) at 12 temperatures ranging from 309.7 to 349.2 K. Each decay was fit with the phenomenological function

$$F(t) = [pt^{-z} + dt^{b-1}]e^{-t/\tau} \quad (3)$$

which has been shown to accurately model the OHD-OKE data for a broad range of liquids including liquid crystals.[26,36−38] The first power law is the "intermediate" power law, and the second power law is the "von Schweidler" power law. These power laws describe cage relaxation, that is, non-Markovian dynamics that occur prior to the long time scale diffusive orientational relaxation. The exponential term describes α relaxation or the final complete orientational randomization of the liquid. For nematogens in the isotropic phase, this exponential decay is called the Landau−de Gennes decay and refers specifically to the randomization of the pseudonematic domains.[26]

Data were fit from 1 ps to near the end of the decay. For both the 5CB samples and 2.5 mol % 5SCB in 5CB samples, the end of the decay varied from 1.00×10^6 ps at 309.7 K to 1.20×10^4 ps at 349.2 K. The 5B samples decayed much more quickly than the nematogen samples, so the decays ended at 4300 ps at 309.7 K and at 1400 ps at 349.2 K.

It was found that both power law exponents were temperature independent in all four samples. Therefore, the

exponents were fixed at the average for all temperatures, and fits were run again. This did not greatly affect the error associated with the fits, which indicated that temperature independence of these parameters was a good assumption. As expected, the exponential time constant was strongly temperature dependent, particularly in the case of the liquid crystal samples. Figure 1

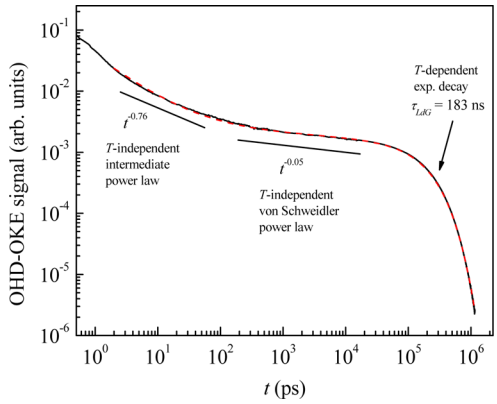

Figure 1. OHD-OKE 5CB data (black solid curve) in the isotropic phase (309.7 K) displayed on a log plot. The longest time component is an exponential decay that is described by Landau−de Gennes theory. At shorter times there are two power laws, the intermediate and von Schweidler power laws. Power laws appear as straight lines on a log plot; lines are drawn below the data to aid the eye. The red dashed curve is a fit to the data using the fitting function, eq 3.

shows OHD-OKE data for 5CB at 309.7 K (black curve) and a fit to the data (red dashed curve) using eq 3. The data cover over four decades of amplitude and six decades of time. Here we are primarily interested in the final exponential LdG decay. However, to obtain an accurate value of the exponential time constant, τ_{LdG}, it is necessary to perform a global fit that includes the power laws. Fits to the data using schematic MCT are presented in section III.E. The MCT fits provide the orientational and density correlation functions.

C. FT-IR Spectroscopy. FT-IR experiments were performed on a Nicolet 6700 FT-IR spectrometer (Thermo-Fisher Scientific) with 1 cm^{-1} resolution. The nitrile absorption bands of 5^{13}CB and 5SCB are centered at 2174 and 2157 cm^{-1}, respectively, in the 5SCB/5CB sample. Both of these peaks are temperature dependent, experiencing a red-shift of approximately one wavenumber as the temperature is increased by 50 K over the range of interest.[21] The nitrile stretch of 5SCB is relatively unchanged in 5B, absorbing at 2157 cm^{-1}. The peak center is temperature independent within the resolution of the spectrometer. Background subtractions of neat 5CB and 5B at the appropriate temperature were performed to isolate the 5SCB nitrile band for data analysis.

D. Ultrafast Infrared Spectroscopy. The experimental setup and methods for these ultrafast infrared experiments have been described in detail in previous publications and are outlined below.[31,39] An optical parametric amplifier (OPA) was pumped by a Ti:sapphire oscillator/regenerative amplifier. The output of the OPA was ∼6 μJ of mid-IR light in ∼150 fs pulses at 1 kHz repetition rate. The center wavelength of the IR was tuned to 2175 or 2160 cm^{-1} for studying 5^{13}CB and 5SCB vibrational probes, respectively. This mid-IR output was split into two beams for pump−probe spectroscopy and four beams for vibrational echo experiments. The timing of pulse arrival at the sample was controlled with precision delay stages with a maximum experimental window of ∼200 ps. The IR spot sizes at the sample were ∼75 μm.

In the pump−probe experiments, by rotating the polarization of the pump pulse relative to the probe, we can extract information on the population relaxation (vibrational lifetime) and orientational dynamics of the sample. The decay of the probe transmission with the polarizations parallel ($I_{\parallel}$) and at the magic angle (I_{ma}) to the pump are given by

$$I_{\parallel} = P(t)(1 + 0.8C_2(t))$$
$$I_{ma} = P(t) \quad (4)$$

where $P(t)$ is the vibrational population relaxation and $C_2(t)$ is the second Legendre polynomial correlation function (orientational correlation function). The measurement of both polarizations permits the extraction of $C_2(t)$ from measurements of $I_{\parallel}$ if the time scale of the orientational relaxation is not significantly longer than the experimental window. The probe (signal) was dispersed by a monochromator and detected by a mercury−cadmium−telluride 32-element array detector.

For vibrational echo experiments, three excitation pulses are crossed in the sample and the fourth pulse serves as a local oscillator (LO). The time between pulses 1 and 2 is the coherence time, τ, and the time between pulses 2 and 3 is the population time, T_w. Nonlinear interactions in the sample between the three excitation pulses produce a fourth pulse, the vibrational echo, which propagates in a unique direction at a time $\leq \tau$ after the third excitation pulse. The LO and vibrational echo are spatially and temporally overlapped to provide heterodyne detection, which amplifies the vibrational echo. Data were collected at a given T_w by scanning the time between pulses 1 and 2; as τ is scanned, the timing of the vibrational echo moves relative to the temporally fixed LO, producing a temporal interferogram. This signal was frequency resolved and detected on the 32-element array, yielding the vertical axis, ω_m, of the 2D IR spectra. By numerically Fourier transforming the interferogram at each ω_m, the horizontal axis, ω_τ, of the 2D IR spectrum was produced. 2D IR spectra were collected at T_w's ranging from 0.5 to approximately 200 ps.

The structural dynamics of a liquid were obtained from the change in shape of the 2D IR spectrum as a function of T_w. The evolution of the shape of the nitrile stretches of 5^{13}CB and 5SCB reports on spectral diffusion. Spectral diffusion, qualitatively explained below, is due to the change in frequency of the CN stretch caused by the structural fluctuation of the medium, either 5CB or 5B here. At any given time, there is a range of CN transition frequencies, causing inhomogeneous broadening in the nitrile absorption band. Homogeneous broadening produces a narrow Lorentzian line shape for each molecule. The collection of all of the narrow Lorentzians with a Gaussian distribution of center frequencies produces the total line shape. Structural evolution of the liquid that influences a given molecule causes its center frequency to change in time, the process known as spectral diffusion. At a sufficiently long time, all possible liquid structures will be sampled by the vibrational probe, causing the nitrile vibration to sample all of the frequencies present in the inhomogeneously broadened absorption spectrum.

The initial and time evolved frequencies of probe molecules are monitored using the vibrational echo pulse sequence. The first and second pulses in effect "label" the initial vibrational frequencies of the nitrile vibrational oscillators. During the population time, T_w, between pulses 2 and 3, the liquid

dx.doi.org/10.1021/jp500144p | J. Phys. Chem. B 2014, 118, 7856−7868

structure can evolve, causing the CN frequencies to change. The arrival of the third pulse ends this time period, and the resulting vibrational echo reports on the nitrile final frequencies. At short T_w, the structure of the liquid has not changed much from when the vibrations were initially labeled. Thus, the read out frequencies are nearly the same as the starting frequencies. As the population time increases, the liquid structure changes more and more; the echo emission frequencies reported by the vibrational echo are decreasingly correlated with their initially labeled frequencies. The manifestations of the decreased correlation as a function of T_w are changes in shape of the 2D IR spectrum. At short T_w, the detection frequency (ω_m) is approximately the same as the excitation frequency (ω_τ), giving a spectrum that is elongated along the diagonal. The shape of the spectrum becomes more symmetrical when the frequencies are less correlated, becoming completely round when all of the environments have been sampled during the population time. In this manner, the rate of structural evolution is observable as the rate of change in the shape of the 2D IR spectra as a function of T_w.

The spectral diffusion amplitudes and time scales are quantified by the frequency−frequency correlation function (FFCF). This function is the joint probability that a vibrational oscillator with an initial frequency in the inhomogeneous spectral distribution will have that same frequency at a later time, averaged over all of the initial frequencies. The FFCF is extracted from the T_w dependence of the shape of 2D spectra using the center line slope (CLS) method.[40,41] The CLS method provides a direct observable that can be plotted to depict the nature of the spectral diffusion dynamics fully described by the FFCF. The CLS as a function of T_w is essentially the normalized decay of the FFCF. Combining the CLS decay with the IR absorption spectrum yields the full FFCF including the homogeneous line width.[40,41]

The FFCF was modeled with the multiexponential form

$$C(t) = \langle \delta\omega_{1,0}(\tau_1)\delta\omega_{1,0}(0)\rangle = \sum_i \Delta_i^2 \exp(-t/\tau_i) \quad (5)$$

where Δ_i and τ_i are the frequency fluctuation amplitude and time constant, respectively, of the ith component. A component, k, of the FFCF with $\Delta_k\tau_k < 1$ is motionally narrowed and a source of the homogeneous broadening in the absorption line. When this occurs, it is not possible to determine Δ_k and τ_k individually. The contribution of the motionally narrowed component of the absorption spectrum has a pure dephasing line width given by $\Gamma^* = \Delta_k^2\tau_k = 1/\pi T_2^*$, where T_2^* is the pure dephasing time. The measured homogeneous dephasing time, T_2, also depends on the vibrational lifetime and orientation relaxation given by

$$\frac{1}{T_2} = \frac{1}{T_2^*} + \frac{1}{2T_1} + \frac{1}{3T_{or}} \quad (6)$$

where T_1 and T_{or} are the vibrational lifetime and orientational relaxation times, respectively.

III. RESULTS AND DISCUSSION

A. OHD-OKE. Previous studies have reported on the OHD-OKE decay of 5CB at a variety of temperatures in the isotropic phase.[10,11,22,23,26] Each decay can be fit with the phenomenological function given in eq 3 and illustrated in Figure 1. The two power law exponents were shown to be independent of temperature, while the final exponential decay is the Landau−de Gennes time constant.[22,23,26] Plotting the viscosity, η, over τ_{LdG} as a function of temperature yields a straight line whose x-intercept is T^*. If 5CB is doped with another substance, the difference in the power law exponents and value of T^* will give a measure of the modification of liquid crystal dynamics from those of pure 5CB.

We collected the OHD-OKE decays of 2.5 mol % 5SCB in 5CB over a range of temperatures above the nematic−isotropic phase transition of 5CB; data for three of the temperatures are shown in Figure 2. As with pure 5CB, each of these doped

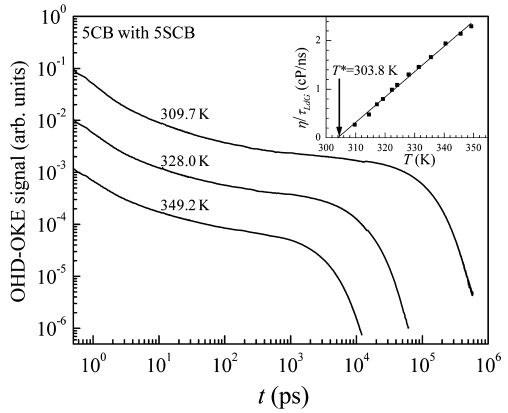

Figure 2. Temperature-dependent 5CB with 2.5 mol % 5SCB OHD-OKE data at three temperatures. The curves have been offset along the vertical axis for clarity. Each decay was fit with the fitting function given by eq 3. The inset shows a Landau−de Gennes plot from the results for the long time exponential decay and viscosity data. The x-intercept of the linear fit gives T^* = 303.8 K for the doped sample of 5CB.

sample decays can be fit with the phenomenological function given by eq 3. The quality of the fits is the same as that shown in Figure 1. Within experimental error, the values of the power law exponents for the doped sample are identical to the pure sample of 5CB (Table 1).[22,23,26] The τ_{LdG} decay constants

Table 1. OHD-OKE Phenomenological Fitting Parameters

sample	z	$b - 1$	τ range (ns)
neat 5CB	0.76 ± 0.02	0.05 ± 0.01	2.7−183
2.5 mol % 5SCB in 5CB	0.78 ± 0.02	0.07 ± 0.02	2.8−95
5B	0.73 ± 0.02	0.15 ± 0.04	0.2−0.7

obtained for 5SCB in 5CB are slightly faster than the neat sample at the same temperatures. This difference is more significant at lower temperatures. Viscosity data for 2.5 mol % 5SCB in 5CB were collected, and a Landau−de Gennes plot of the doped sample was constructed. As seen in the inset of Figure 2, the doped sample of 5CB obeys Landau−de Gennes theory, as η/τ_{LdG} versus temperature is well fit by a line as is pure 5CB. The x-intercept of this line is 303.8 K, approximately 3 K lower than that of pure 5CB.

The doped sample of 5SCB in 5CB maintains the liquid crystal nature of the sample but with an ∼1% lower critical temperature. This is in accordance with other studies that show that the introduction of small amounts of impurity into 5CB lowers the nematic−isotropic phase transition temperature.[42,43] The vibrational probe, 5SCB, is very similar in shape to 5CB. The agreement in the power laws of the OHD-OKE decays is evidence that the presence of 5SCB does not significantly

dx.doi.org/10.1021/jp500144p | J. Phys. Chem. B 2014, 118, 7856−7868

change the dynamics within the pseudonematic domains. The sizes of the pseudonematic domains themselves are equivalent to those in neat 5CB at a slightly higher temperature. Thus, we can study the spectral diffusion of the 5SCB probe in 5CB without substantially perturbing the liquid crystal nature of 5CB.

To explicate the dynamics due to the presence of pseudonematic domains, we have studied 5B, a liquid that is molecularly similar to 5CB, but not a nematogen.[33] OHD-OKE experiments were conducted on 5B at the same temperatures as the doped sample of 5CB. Note, these temperatures are all well above the melting point of 5B at 10 °C, so it is not supercooled.[44,45] The OHD-OKE decays observed for 5B at selected temperatures are shown in Figure 3. These data do not

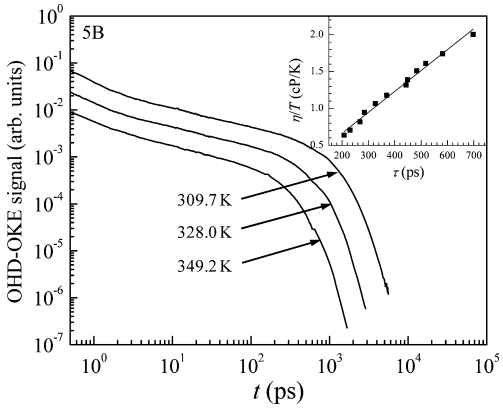

Figure 3. Temperature-dependent 5B OHD-OKE data at three temperatures. The curves have been offset along the vertical axis for clarity. Each decay was fit with the fitting function given by eq 3. The inset shows a Debye–Stokes–Einstein plot from the resulting final exponential decay constants and viscosity data. As η/T versus τ is linear, 5B obeys Newtonian fluid mechanics (Debye–Stokes–Einstein rotational diffusion) consistent with a normal liquid, not a nematogen.

have 5SCB in them, but the decays for 5B with 5SCB are identical within experimental error. The 5B decays are substantially faster than those for 5CB. As with neat and doped 5CB, these decays can be fit to two power laws times an exponential (eq 3). Again, the power law exponents are independent of temperature; their values are reported in Table 1. The values of these exponents for 5B are similar but not the same as those for 5CB. The z exponent is almost within the error bars of the 5CB value, but the b exponent is different. However, the uncertainty in the 5B values is larger because the final exponential decays are much faster, limiting the range of time over which the power laws can be observed. The slowest of the final exponential relaxations observed for 5B is faster than 1 ns; the fastest of the 5CB Landau–de Gennes time constants is still significantly slower. In addition to being faster overall, the 5B final exponential decay constant is less sensitive to temperature changes. It changes by a factor of ~2 over the range of temperatures examined, while τ_{LdG} for 5CB changes by more than a factor of 80. The difference in the temperature dependences is expected, as the long time orientational relaxation dynamics in 5CB are dominated by the orientational randomization of pseudonematic domains, which are absent in 5B. Finally, it is worth noting that the long time exponential decay constants of 5B obey Debye–Stokes–Einstein behavior for Newtonian fluids, as seen in the inset of Figure 3.

B. Linear Infrared Spectroscopy. The nitrile stretch absorption of 5SCB is located at ~2157 cm^{-1} in both 5B and 5CB. While 5B is essentially void of peaks in the region, 5CB has absorptions from both the carbon-12 and carbon-13 nitrile stretches. The nitrile absorption from 5SCB cannot be completely isolated from the CN peaks of 5CB, but the signals can be separated in the 2D IR experiments.[21]

As was observed for 5^{12}CB and 5^{13}CB previously, the center frequency of the nitrile stretch of 5SCB is slightly temperature dependent.[21] The peak center shows a red-shift with increasing temperature in 5CB. However, in 5B, no center frequency shift is observed with temperature changes. In both liquids, the nitrile absorption of 5SCB shows as a slight broadening with increased temperature.

C. Polarization Selective Pump–Probe Spectroscopy. Magic angle pump–probe experiments at four temperatures were conducted for 5SCB in both 5B and 5CB and are shown in Figure 4. The magic angle population decay of the nitrile

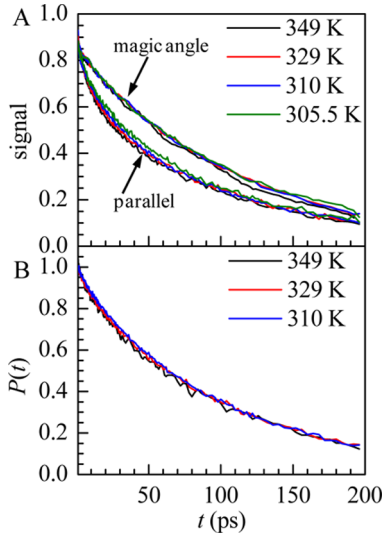

Figure 4. Polarization selective pump–probe decays for 5SCB in 5B (A) and in 5CB (B). The signal decay for both magic angle and parallel are shown for 5SCB in 5B. The parallel pump–probe signal for 5SCB in 5CB is identical to the magic angle, so it is not shown. The fits are not shown to avoid clutter.

absorption of 5SCB in 5B, Figure 4A, was fit with a single exponential to give the vibrational lifetime; the lifetime is ~105 ps and increases slightly with decreasing temperature (see Table 2). In 5CB, the population decay of the 5SCB nitrile absorption was fit with a biexponential decay, Figure 4B. The first of the exponential time constants is due to the somewhat

Table 2. Vibrational Lifetimes T_1

probe	liquid	temperature (K)	T_1 (ps)
5SCB	5CB	349	101 ± 1
5SCB	5CB	329	103 ± 1
5SCB	5CB	310	101 ± 1
5SCB	5CB	305.5	100 ± 2
5SCB	5B	349	103 ± 1
5SCB	5B	329	108 ± 1
5SCB	5B	310	108 ± 1
5SCB	5B	305.5	111 ± 1

dx.doi.org/10.1021/jp500144p | J. Phys. Chem. B 2014, 118, 7856–7868

overlapping 5^{13}CB 1−2 transition and is small in amplitude. It is held fixed at the temperature dependent lifetime values found for 5^{13}CB in neat 5CB. The longer exponential decay constant is the vibrational lifetime of the nitrile stretch of 5SCB, ∼101 ps. Within experimental error, the lifetime of the 5SCB nitrile stretch in 5CB is independent of temperature (see Table 2). A precise value cannot be obtained at 305.5 K, as neat 5CB is in the nematic phase at this temperature; thus, we cannot fix the value of the fast exponential to the lifetime of 5^{13}CB.

Pump−probe experiments with parallel geometry were performed on the same samples to extract information on the orientational relaxation. At each temperature, the parallel pump−probe decay of the nitrile stretch of 5SCB in 5CB was found to be identical to the magic angle decay, which demonstrates that no significant orientational relaxation occurs on the time scale of the pump−probe experiment, approximately 200 ps. As discussed in detail below, examining the first 200 ps of the orientational correlation function found from schematic MCT fitting of the OHD-OKE data shows that its decay is exceedingly slow. The orientational correlation function drops from 1 to ∼0.96 in the span of the pump−probe experiments; thus, orientational relaxation is not observed in the parallel pump−probe experiments.

Unlike in 5CB, the population decay of nitrile stretch of 5SCB in 5B in parallel pump−probe experiments can be distinguished from the magic angle decay, Figure 4A, and it can be fit with a biexponential decay. The longer of these two exponential decay constants matches the magic angle vibrational lifetime of the nitrile stretch of 5SCB in 5B. The faster time constants are 10−20 ps over the range of temperatures studied, and may be related to the rotation of the transition dipole of 5SCB around the long axis of the molecule. Full anisotropy measurements are required for a complete characterization and will be undertaken in future experiments.

D. 2D IR Vibrational Echo Experiments. In a previous paper, it was shown in detail that the introduction of 5SCB does not change the structural dynamics (spectral diffusion) in 5CB measurements at a single temperature. The measurements were made using 5^{13}CB as the vibrational probe with and without 5SCB in the liquid.[21] In addition, the dynamics in 5CB were measured using both 5^{13}CB and 5SCB as vibrational probes. As mentioned above, the ^{13}CN stretch has a vibrational lifetime of ∼8 ps, while the CN stretch of 5SCB has a lifetime of ∼100 ps. The spectral diffusion, quantified by the CLS decays, was the same for 5^{13}CB and the CN stretch of 5SCB over the 25 ps window that could be measured for 5^{13}CB given its relatively short lifetime. There may be a small difference in the homogeneous line width.[21] In this study, the measurements were repeated at the temperatures used in here, and the results are the same. The CLS decays measured on 5^{13}CB with and without 5SCB are the same, and over the time range limited by the ^{13}CN stretch lifetime of 5^{13}CB, the spectral diffusion of 5^{13}CB and 5SCB is the same.

Unlike 5CB, 5B does not contain an intrinsic vibrational probe. Thus, we cannot compare the dynamics reported by the CN stretch of 5SCB to anything already present in the solution. On the basis of the identical OHD-OKE decays of neat 5B and 5SCB doped 5B, it is assumed that the introduction of 5SCB does not greatly perturb the 5B liquid dynamics and that the nitrile stretch of 5SCB can accurately report on its structural evolution.

Figure 5 displays 2D IR spectra of the CN stretch of 5SCB in 5CB at 349 K. The top panel is the spectrum for a short T_w = 1 ps, and the bottom panel is for a long T_w = 168 ps. Structural fluctuations of the liquid cause spectral diffusion, which is manifested as changes in the shape of the 2D IR spectra. In the top panel, the dashed line is the diagonal. At short time, the spectrum is elongated along the diagonal. The width perpendicular to the diagonal at short time is related to the homogeneous line width. At the long time shown in the bottom panel, the spectrum is virtually symmetrical (circular), which reflects almost complete spectral diffusion. Complete spectral diffusion means that all frequencies in the inhomogeneously broadened absorption line have been sampled because all liquid structures that are responsible for the inhomogeneous broadening have been sampled.

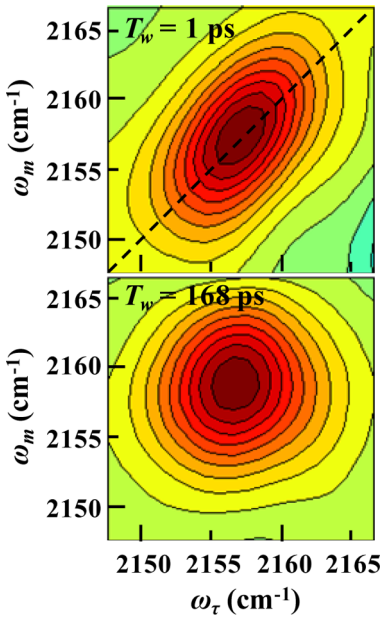

Figure 5. 2D IR spectra of the CN stretch of 5SCB in 5CB at 349 K. The top panel is the spectrum for a short T_w = 1 ps, and the bottom panel is for a long T_w = 168 ps. The dashed line in the top panel is the diagonal. Information of spectral diffusion is contained in the change in shape of the spectra with time.

Parts A and B of Figure 6 show the CLS decays at four temperatures for the nitrile stretch of 5SCB in 5B and 5CB, respectively. The differences in the CLS decays in the two liquids are not large considering the very large differences in the decays of the OHD-OKE data for the two liquids (see Figures 2 and 3). At 310, 329, and 349 K, the CLS decays are fit very well to a triexponential function for both liquids. Fits with biexponential functions do not give a reasonable description of the data. The Akaike statistical analysis[46] was applied to compare the biexponential and triexponential fits. The analysis demonstrated that the triexponential function is appropriate. The 5B and 5CB time constants for the decays are very similar, as seen in Table 3. Note that at each temperature for a particular liquid the three time constants differ by factors of 5−10, again supporting the triexponential fit. There is a substantially smaller homogeneous line width at these temperatures for 5CB than in 5B. Two of the inhomogeneous amplitudes, Δ_1 and Δ_2, are similar for the two liquids, while Δ_3 is significantly larger for 5CB.

On the basis of CLS decays down to 310 K, there are no significant differences between the structural evolution of 5B and 5CB that would suggest the presence of pseudonematic domains in 5CB is sensed by the vibrational probe. The 2D IR

dx.doi.org/10.1021/jp500144p | J. Phys. Chem. B 2014, 118, 7856−7868

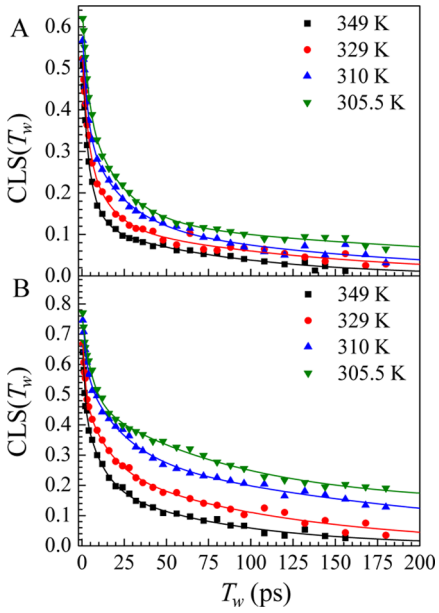

Figure 6. (A) The 2D IR CLS data (points) for 5SCB in 5B at 349, 329, 310, and 305.5 K. Each curve is fit to a triexponential decay with no offset (solid curves). The resulting FFCF parameters are given in Table 3. (B) The 2D IR CLS data (points) for 5SCB in 5CB at 349, 329, 310, and 305.5 K. Fits to the data are the solid curves. The CLS decays for the three higher temperatures (black, red, and blue) were fit to a triexponential with no offset. The CLS decay at 305.5 K is fit with a biexponential with an offset (see text). The FFCF parameters are given in Table 3.

measurements on individual probe molecules do not display evidence of the presence of pseudonematic domains in 5CB, in sharp contrast to the OHD-OKE experimental results shown in Figures 2 and 3, which display marked differences between the 5CB and the 5B data. OHD-OKE experiments measure orientational relaxation through randomization of the pseudonematic domains in 5CB but normal orientational relaxation in 5B. The 2D IR experiments measure the dynamics of the structures that give rise to the inhomogeneously broadened absorption lines. The results for the three highest temperatures indicate that complete orientational relaxation is not necessary for randomization of the structures responsible for inhomogeneous broadening. The relationship between the 2D IR experiments and the OHD-OKE experiments is discussed in detail below.

For the four temperatures studied, 349, 329, 310, and 305.5 K, the correlation lengths, ξ, of the pseudonematic domains are 1, 1.4, 2.8, and 5.4 nm, respectively, as calculated using eq 1. Here, we have taken ξ_0 to be 4 Å, in accordance with previous studies on *n*-cyanobiphenyls.[3,4] For the highest three temperatures, the correlation lengths are not insignificant, but the 310 K value of 2.8 nm is still only about double the long molecular axis of 5CB. It is not until the temperature is held very close to T^* that ξ grows dramatically. To examine the maximum impact of these pseudonematic domains on spectral diffusion, we conducted 2D IR experiments at 305.5 K, very close to the phase transition for 5CB containing 5SCB (see Figure 6B).

At 305.5 K, the sample is less than 2 K above T^*, and the correlation length is 5.4 nm. Compared to the sample held at 310 K, just 4.5 K higher, we see a doubling in ξ. It is at this temperature that substantial differences in the nature of the spectral diffusion in 5B versus 5CB were observed. The faster two components of the dynamics in 5B at 305.5 K, τ_1 and τ_2, do not change within experimental error going from 310 to 305.5 K. The slowest component for 5B, τ_3, becomes slower by about a factor of 2 but has a large associated uncertainty (see Table 3). The functional form of the decay is still a triexponential without an offset; that is, the slowest component will take the CLS to zero. Unlike in the "normal" liquid 5B, the spectral diffusion of the 5SCB probe in the nematogen liquid 5CB exhibits dramatic slowing at 305.5 K. For 5CB, τ_1 becomes approximately a factor of 3 longer and τ_2 becomes approximately a factor of 4 longer (see Table 3). Furthermore, τ_3 becomes so slow that we cannot measure it within the experimental time window of 180 ps. The data can be fit with the triexponential function, but the long component goes to infinity. Alternatively, the 305.5 K 5CB data can be fit with a biexponential with an offset. The offset reflects a constant value in terms of the data. The net result is the same. The two decay time constants that can be measured become much slower, and the slowest time constant also becomes much slower but too slow to obtain a numerical value.

These results demonstrate that the presence of pseudonematic domains does influence the structural dynamics reported by spectral diffusion but only when the correlation length of the domains becomes very large near the nematic–isotropic phase transition temperature. The 2D IR experiments are in contrast to the OHD-OKE data, for which the correlation length has a major influence on the orientation relaxation of 5CB for all correlation lengths.

Table 3. FFCF Parameters for 5SCB in 5B and 5CB

sample	T (K)	$\Delta_1{}^a$ (cm^{-1})	τ_1 (ps)	$\Delta_2{}^a$ (cm^{-1})	τ_2 (ps)	$\Delta_3{}^a$ (cm^{-1})	τ_3 (ps)	T_2 (ps)	Γ (cm^{-1})
5B	349	1.67 ± 0.2	1.9 ± 0.5	1.79 ± 0.2	7 ± 1	1.31 ± 0.2	84 ± 5	3.13 ± 0.3	3.39 ± 0.3
	329	1.67 ± 0.2	2.7 ± 0.7	1.62 ± 0.2	13 ± 4	1.28 ± 0.2	131 ± 23	3.25 ± 0.3	3.27 ± 0.3
	310	1.75 ± 0.2	2.9 ± 0.5	1.68 ± 0.2	22 ± 6	1.29 ± 0.2	163 ± 50	3.44 ± 0.3	3.09 ± 0.3
	305.5	1.69 ± 0.2	3.2 ± 0.4	1.90 ± 0.2	21 ± 3	1.29 ± 0.2	310 ± 71	3.86 ± 0.4	2.75 ± 0.3
5CB	349	2.04 ± 0.2	1.1 ± 0.3	2.08 ± 0.2	10 ± 2	1.83 ± 0.2	78 ± 9	3.80 ± 0.4	2.79 ± 0.3
	329	1.84 ± 0.2	1.6 ± 0.4	1.94 ± 0.2	14 ± 4	2.06 ± 0.2	111 ± 12	4.21 ± 0.4	2.52 ± 0.25
	310	1.79 ± 0.2	2.2 ± 0.4	2.08 ± 0.2	22 ± 4	2.19 ± 0.2	221 ± 31	5.85 ± 0.6	1.81 ± 0.2
	305.5	2.13 ± 0.2	5.7 ± 0.8	2.35 ± 0.2	87 ± 16	1.49 ± 0.2		5.83 ± 0.6	1.83 ± 0.2

[a]The Δ_i values are the standard deviations of the ith component of the inhomogeneous contribution to the absorption line. The standard deviation of the total inhomogeneous line width is $(\sum_i \Delta_i^2)^{1/2}$. The full width at half-maximum (fwhm) of the inhomogeneous component of the absorption line is 2.35 times the standard deviation of the total inhomogeneous component. The fwhm of the total absorption spectrum is the convolution of the fwhm of the homogeneous line width, Γ, with the fwhm of the inhomogeneous component. The total absorption line shape is a Voigt profile.

dx.doi.org/10.1021/jp500144p | J. Phys. Chem. B 2014, 118, 7856–7868

E. Schematic MCT Fitting of OHD-OKE Decays and the Relation to 2D IR. The detailed analysis of the results of the OHD-OKE experiments can be used to clarify the nature of the structural dynamics that are responsible for the spectral diffusion measured with the 2D IR experiments. In addition to the analysis of OHD-OKE data with the phenomenological fitting function given by eq 3, the data for the nematogen liquid 5CB and nonmesogenic 5B have been described quantitatively using schematic mode coupling theory. A full description of schematic MCT can be found elsewhere,[27,28,47,48] as well as its extension to nematogens in the isotropic phase.[23] In the Sjögren model of schematic MCT, there are two coupled correlation functions. Here $\phi_1(t)$ is associated with the density fluctuations, and $\phi_2(t)$ is associated with the orientational fluctuations.[23,28,47] The derivative of the orientational correlation function gives the OHD-OKE experimental decay. To accommodate the divergence of the long time exponential behavior of the nematogen 5CB as T^* is approached from above, a modified version of schematic MCT is employed, given by[23]

$$\ddot{\phi}_1(t) + \mu_1\dot{\phi}_1(t) + {\Omega_1}^2\phi_1(t) + {\Omega_1}^2\int_0^t d\tau m_1(t-\tau)\dot{\phi}_1(\tau) = 0$$

$$\ddot{\phi}_2(t) + (\mu_2 + \Gamma)\dot{\phi}_2(t) + ({\Omega_2}^2 + \mu_2\Gamma)\phi_2(t) + {\Omega_2}^2\int_0^t d\tau m_2(t-\tau)\dot{\phi}_2(\tau) + {\Omega_2}^2\Gamma\int_0^t d\tau m_2(t-\tau)\phi_2(\tau) = 0 \quad (7)$$

where the memory kernels are

$$m_1(t) = \nu_1\phi_1(t) + \nu_2{\phi_1}^2(t)$$

$$m_2(t) = \kappa\phi_1(t)\phi_2(t) \quad (8)$$

and Γ is the inverse of the Landau−de Gennes time constant in the case of 5CB or 0 in the case of 5B.[23] The equations are damped harmonic oscillators with memory functions. Ω_1 and Ω_2 are the microscopic oscillator frequencies and μ_1 and μ_2 are the oscillator damping constants for the density and orientational correlation function equations, respectively. ν_1 and ν_2 are the magnitudes of the linear and quadratic terms in the density memory kernel, and κ is the constant that reflects the magnitude of the coupling of the orientational relaxation to the density relaxation. These equations cannot be solved analytically, and the numerical solution for a time point N depends on the solution at all previous time points. The procedure outlined below was employed for fitting the data.

The OHD-OKE decays were fit from 1 ps to an end point ranging from 1 ns to 1 μs as determined by the duration of the final exponential decay. As the schematic MCT equations contain a total of eight free parameters that are possibly temperature dependent, some restrictions had to be made to fit the data. In accordance with previous studies, the microscopic oscillator frequencies Ω_1 and Ω_2 were taken to be temperature independent.[23,28,36,47] Fitting data with the remaining six freely adjustable parameters resulted in density damping constant, μ_1, values that were also essentially temperature independent; this temperature independence is in agreement with previous results for liquid crystals and molecular liquids well above the glass transition.[23,28] Setting μ_1 to be the average of the values found at all temperatures, the data were refit to obtain the temperature dependent values for the other damping constant, μ_2, the F_{12} parameters, ν_1 and ν_2, and the density-orientational coupling constant, κ.

The numerical method involved in solving the coupled differential equations is dependent on the time point step size. It is necessary to use a fine point spacing at early times (power law region) and desirable to use a larger point spacing at later times (final exponential decay). When the step size is changed, a discontinuity appears in the resulting fit. This discontinuity is negligible when $\Gamma = 0$ in the case of 5B. However, when Γ is nonzero for 5CB, these jumps in the fit severely skew the parameters. Thus, the step size must be kept constant at a small value, 0.5 ps, throughout the fit. While this produces a well behaved result, the fitting takes a very long time, since a vast number of points are needed, and the time for a fit scales approximately as the number of points squared. Therefore, only a few temperatures of 5CB OHD-OKE data are fit and presented as results.

For both 5B and 5CB, the oscillator frequencies Ω_1 and Ω_2 were held constant at 0.5 and 1 THz in accordance with previous works.[28,36,47] Choosing smaller values results in short time oscillations in the OHD-OKE fit, while larger values result in oscillator energies in the regime of bond vibrations. Additionally, ν_1 and ν_2 were found to be effectively temperature independent in the two liquids. Figure 7 shows OHD-OKE data for 5CB with 5SCB at T = 328 K (solid black curve) and the MCT fit (dashed red curve). The data span more than three decades in amplitude and more than four decades in time. The fit is excellent over the entire time range. The quality of the fits is the same at all temperatures and for 5B with and without 5SCB as well.

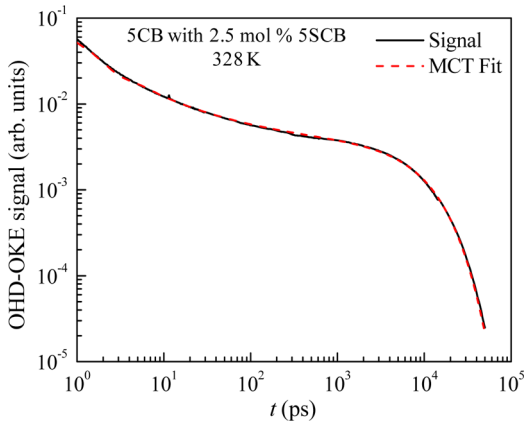

Figure 7. OHD-OKE data (solid black curve) for 5CB with 5SCB at 328 K and the MCT fit to the data (dashed red curve). Fixed parameters: Ω_1 = 0.5 THz, Ω_2 = 1 THz, μ_1 = 1.19 THz, ν_1 = 0.99, ν_2 = 0.3, $\Gamma = 9.7 \times 10^{-5}$ ps^{-1}.

It has been shown previously for three nematogens including 5CB that, as T^* is approached from above, κ, the constant for the coupling of the orientational correlation function to the density correlation function, diverges.[23] A plot of $1/\kappa$ vs T falls on a line, and the intercept is T^* within experimental error.[23] Figure 8 shows plots of $1/\kappa$ vs T for neat 5CB (red points) and 5CB with 2.5 mol % 5SCB (blue points). The lines through the data are linear fits. As previously reported, the neat 5CB data falls on a line. The data taken in this study has an intercept of ~309.5 K, which is close to T^* = 308 K. The data for 5CB with 2.5 mol % 5SCB also falls on a line with an intercept of ~306 K, which is close to the mixed sample's T^* = 304 K. The only difference between the doped sample and pure 5CB is a reduction of T^* of about 4 K. The results displayed in Figure 8

dx.doi.org/10.1021/jp500144p | J. Phys. Chem. B 2014, 118, 7856−7868

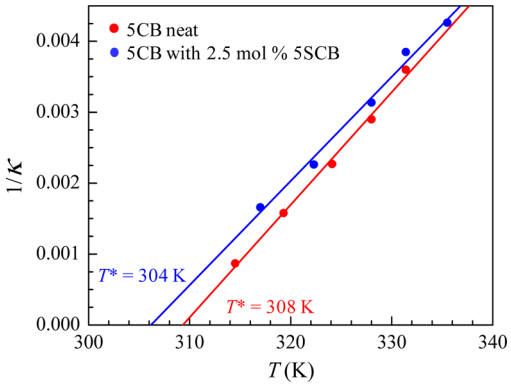

Figure 8. Plots of $1/\kappa$ vs temperature obtained from the MCT fits (points) and linear fits (lines) for pure 5CB (red) and 5CB with 2.5 mol % 5SCB (blue). Within experimental error, the intercepts are T^*, as found from OHD-OKE experiments, for the two liquids.

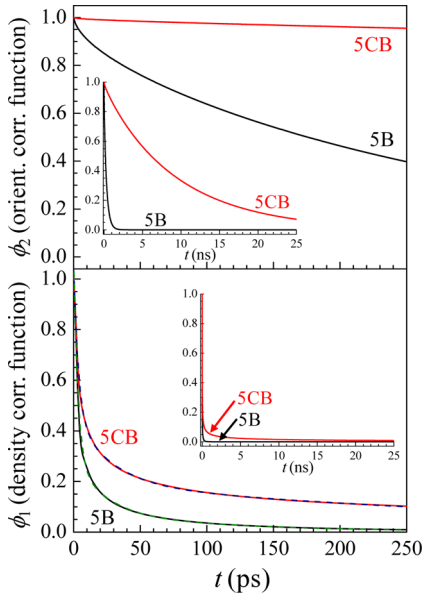

Figure 9. Plots of the orientational correlation functions (top panel) and the density correlation functions (bottom panel) for 5CB (red) and 5B (black) both with 2.5 mol % 5SCB obtained from MCT fits to the data at 328 K. The time axes for the main figures are in picoseconds, while the insets are in nanoseconds. The density correlation functions (bottom panel) also have triexponential fits (dashed curves).

show that, as the isotropic to nematic phase transition is approached from above, the coupling of the orientational relaxation to the density relaxation grows dramatically and diverges at T^*. In the LdG theory, the correlation length grows and becomes infinite at T^*. MCT indicates that the divergence of the correlation length is accompanied by the divergence of the coupling of the orientational relaxation to the density relaxation. For the nonmesogenic 5B, κ does not diverge, which agrees with MCT analysis of supercooled and ionic liquids.[28,36]

While complete analysis of the fitting parameters of schematic MCT may provide interesting temperature dependences worth studying in the future, our current focus is on the density and orientational correlation functions, $\phi_1(t)$ and $\phi_2(t)$, that are produced from fitting the OHD-OKE data. Although there are many parameters, they are limited to certain ranges or it is not possible to fit the OHD-OKE data. As shown in Figure 7, schematic MCT fits the data exceedingly well. The fit is the derivative of the orientational correlation function; therefore, the shape of the orientational correlation function obtained from the fit is also correct at each temperature. We also examined the shape of the density correlation function. Changing the fixed parameters and then fitting the OHD-OKE data again to produce an excellent fit does not change the shape of the density correlation function. Therefore, although there is a range of parameters that can give good fits, the actual shapes of the density and orientational correlation functions are unchanged and can be examined.

For the present discussion, we will consider the OHD-OKE decays of 5CB and 5B, both with 2.5 mol % 5SCB at 328 K, approximately 25 K above T^*. Figure 9 displays the orientational correlation functions, ϕ_2 (top panel), and the density correlation functions, ϕ_1 (bottom panel), obtained from the fits to the OHD-OKE data (see Figure 7). Note that the time scale for the main portion of each figure is in picoseconds, while the insets are in nanoseconds. First, consider the correlation functions for 5CB (red curves). The CLS for the 5CB sample at 329 K decays almost to zero by 200 ps (see Figure 6B). The orientational correlation function for 5CB (top panel) decays very slowly, dropping only a few percent over the first 200 ps. The inset in Figure 9 shows it has still not decayed to zero at 25 ns. Therefore, the orientational relaxation dynamics are far too slow to account for the structural fluctuation induced spectral diffusion shown in Figure 6 with the FFCF parameters given in Table 3. In contrast, the density correlation function for 5CB (bottom panel) does decay on the appropriate time scale. From this comparison of the orientational and density correlation function decays to the FFCF decay, we can conclude that orientational dynamics are not responsible for the spectral diffusion. The results suggest that spectral diffusion is dominated by density fluctuations. Since the spectral diffusion samples virtually the entire inhomogeneously broadened 5SCB absorption line by 200 ps, the implication is that the inhomogeneous broadening is caused by density variations rather than orientational variations.

Now consider the correlation functions for 5B (black curves in Figure 9). The orientational correlation function decay (top panel) is much faster than that of 5CB, which would be expected for a nonmesogenic liquid. Although the decay is fast compared to 5CB, it is still relatively slow compared to the CLS decay for 5B at 329 K shown in Figure 6A. By 200 ps, the CLS has decayed virtually to zero. Therefore, it is likely that the structural fluctuation induced spectral diffusion for 5B is dominated by density fluctuations but possibly with a non-negligible contribution from orientational fluctuations.

The CLS (Figure 6) and the FFCFs (Table 3) for both the 5CB and 5B samples are described very well by triexponential functions. As a heuristic exercise, it is informative to fit the density correlation functions with triexponentials. The bottom panel of Figure 9, which shows the 5CB (red solid curve) and 5B (black solid curve) density correlation functions also has the triexponential fits: 5CB blue dashed curve and 5B green dashed curve. The fits are very good, demonstrating that the density correlation functions can be fit with the same functional form used to fit the CLS curves. The time constants for the fit to the 5CB density correlation function are 3.5, 27.2, and 382 ps. These should be compared to the FFCF time constants for 5CB at 329 K given in Table 3. The two fast FFCF time constants are approximately a factor of 2 too fast, and the

dx.doi.org/10.1021/jp500144p | J. Phys. Chem. B 2014, 118, 7856−7868

slowest time constant is about a factor of 3.5 too fast. While the density correlation function does not reproduce the spectral diffusion decay precisely, it is certainly in the correct time range. The time constants for the fit to the 5B density correlation function are 3.2, 23.2, and 116 ps. These values are actually quite close to the corresponding FFCF values for 5B at 329 K. These results support the proposition that density fluctuations are primarily responsible for the spectral diffusion measured with the 2D IR experiments.

While there is no a priori reason why the time dependence of the density correlation functions should correspond directly to the spectral diffusion dynamics, a couple of comments are worth making. First, for many vibrations, the change in vibrational frequency with density is linear for small changes.[49] Since spectral diffusion results from frequency fluctuations, there could be a direct correspondence. Second, the agreement between the time dependence of the density correlation function and the FFCF is much better for 5B than for 5CB. The MCT theory for 5B is the standard method for describing a normal liquid.[28,47] The MCT theory of the nematogen 5CB is a modified form to account for the isotropic to nematic phase transition.[23] However, to account for the nematogen OHD-OKE data, which observes orientational dynamics, only the orientational component of the MCT theory was modified; that is, only the equation for ϕ_2 was changed.[23] The changes to the ϕ_2 equation were sufficient to reproduce the OHD-OKE data. In the nematogen MCT theory, the density correlation function equation for ϕ_1 is identical to that of a normal liquid. The results presented here suggest that a modified form of the ϕ_1 equation may also be necessary to completely describe nematogens in the isotropic phase. The problems with the nematogen MCT theory are further indicated, as it does not have the correct temperature dependence. The density correlation function does not display the very large change seen in the 2D IR data very close to T^*, which is reasonable as there is nothing in the ϕ_1 equation that corresponds to the isotropic to nematic phase transition.

F. The Correlation Length and Spectral Diffusion. The results presented above provide some insights into the influence of the correlation length of the pseudonematic domains of 5CB on the spectral diffusion of the 5SCB vibrational probe. Spectral diffusion is produced by fluctuations of the environment that cause the transition frequency of the vibrational probe to evolve through the frequencies of the inhomogeneously broadened IR absorption line. The results of the MCT fits to the OHD-OKE data provide strong evidence that the orientational relaxation is far too slow to contribute to the spectral diffusion and suggests that spectral diffusion is the result of density fluctuations. At all but the lowest temperature, the CLS decays to zero on the hundreds of picosecond time scale. For the CLS to decay to zero, it is necessary for all structures that contribute to the inhomogeneous line to be sampled. The inhomogeneous line width is $(\sum_i \Delta_i^2)^{1/2}$, where the Δ_i are given in Table 3. Within experimental error, the inhomogeneous line width does not change with temperature. These considerations indicate that the inhomogeneous line is a result of variations of the density experienced by the vibrational probe.

As discussed in section III.D, the 2D IR experiments show that the temperature dependences of the spectral diffusion are very similar for 5CB and the nonmesogenic liquid 5B, and the actual spectral diffusion time constants for the two liquids are very similar (see Table 3) at the higher temperatures. It is only at the lowest temperature, which is close to T^*, that the dynamics of 5CB are substantially different from those of 5B. The implication is that, when the correlation length is relatively short, the manner in which structural fluctuations impact the vibrational transition frequency is basically the same for 5CB and 5B. The presence of pseudonematic domains with relatively short correlation lengths in the isotropic phase of the nematogen liquid 5CB is inconsequential, which is in contrast to the orientational relaxation. The orientational relaxation is strongly affected by the pseudonematic domains at all temperatures (see Figures 2 and 3), and the forms of the temperature dependences are fundamentally different for 5CB and 5B.

The substantial slowing of the spectral diffusion in 5CB compared to 5B near T^* is associated with the correlation length becoming large. This is an interesting phenomenon. The nature of structural fluctuations experienced by the local vibrational probe, 5SCB, changes when ξ becomes large, but orientational relaxation is too slow to be involved. This line of argument implies that long-range angular correlation slows the decay of the structural fluctuations responsible for spectral diffusion, and these structural fluctuations may be associated with density fluctuation.

IV. CONCLUDING REMARKS

Ultrafast 2D IR vibrational echo spectroscopy and optical heterodyne detected optical Kerr effect experiments combined with schematic mode coupling theory were used to investigate the dynamics in the isotropic phase of the nematogen 5CB and a related nonmesogenic liquid, 5B. The 2D IR experiments were conducted on a dilute vibrational probe, 5SCB, which has a long lifetime, and it was shown that the structural dynamics of 5CB are not significantly perturbed by the presence of the probe. The isotropic phase of a nematogen liquid undergoes orientational relaxation that is strongly influenced by the existence of pseudonematic domains. On a distance scale characterized by the correlation length, ξ, the nematogen molecules have quasi-nematic order. As the isotropic to nematic phase transition temperature is approached from above, ξ grows and becomes infinite below the transition temperature. As ξ becomes larger, orientational relaxation slows dramatically.

The results presented above demonstrate that the presence of pseudonematic domains has little impact on spectral diffusion measured with the 2D IR experiments until ξ becomes very large close to T^*. Spectral diffusion is caused by fluctuations of the liquid structures that give rise to the inhomogeneously broadened IR absorption line of the vibrational probe. For the higher temperatures studied, the temperature dependences of 5CB and 5B are very similar; the actual spectral diffusion time constants of the two liquids are almost the same at each temperature. However, very close to T^*, where $\xi > 5$ nm, the spectral diffusion of 5CB is much slower than that of 5B. MCT analysis of the OHD-OKE data suggests that the spectral diffusion is caused by density fluctuations and that, for 5CB, orientational fluctuations make little or no contribution.

The behavior of 5CB is fundamentally different than other systems with a nanoscopic dimension that influences dynamics. A wide variety of systems have a nanoscopic dimension that involves an interface of some type, such as water molecules at the surface of a protein or water in nanoscopic water pools of reverse micelles. In AOT reverse micelles with water pool radii of 1 nm, all of the water molecules are affected by the presence

of the AOT interface.[12] When the radii are 5 nm, much of the water behaves like bulk water, although the water molecules very close to the interface are still strongly affected by the presence of the interface. 5CB provides the opportunity to study the influence of a nanoscopic length scale on a single component system. There is no interface but rather a correlation length. 5CB behaves in the exact opposite manner of systems that have a nanoscopic scale defined by an interface. In 5CB, when the correlation length is small, 1 or 2 nm, the presence of the pseudonematic domains has no discernible effect on the structural dynamics that sample the configurations that produce the vibrational probe's inhomogeneous line, although the existence of the pseudonematic domains does strongly influence the orientational dynamics. Only when the correlation length becomes large are the spectral diffusion dynamics different from those of a similar nonmesogenic liquid. These results show that there is a major difference between a system that has an intrinsic length scale not associated with the proximity to an interface and systems that are nanoscopic because of an interface.

From the results presented here, the question arises as to the details of the temperature dependent spectral diffusion close to T^*. At the present time, we are unable to resolve the slowest component in the CLS decay near T^*; it appears as an offset. In the future, we will conduct 2D IR experiments with 4-pentyl-4′-selenocyanobiphenyl (5SeCB) as the vibrational probe. The introduction of a heavier blocking atom, selenium, has been shown to increase the vibrational lifetime of a CN stretch to ∼300 ps.[50] Our preliminary experiments show that the CN lifetime of 5SeCB is longer than 300 ps. The longer lifetime combined with the installation of a longer delay line will enable us to measure the spectral diffusion in 5CB and other nematogenic liquids to >1 ns. With the ability to quantify spectral diffusion at temperatures close to T^*, it may be possible to determine a critical correlation length that impacts the structural evolution observed with 2D IR experiments. Comparison of 2D IR results on 5SeCB in 5CB in the nematic phase will provide further insights into the influence on dynamics of the inherent long-range ordering of rod-like nematogens.

AUTHOR INFORMATION

Corresponding Author

*E-mail: fayer@stanford.edu.

Notes

The authors declare no competing financial interest.

ACKNOWLEDGMENTS

This work was funded by the Division of Chemistry, Directorate of Mathematical and Physical Sciences, National Science Foundation Grant No. CHE-1157772. K.P.S. thanks Stanford University for a Graduate Research Fellowship.

REFERENCES

(1) de Gennes, P. G.; Prost, J. *The Physics of Liquid Crystals*; Clarendon Press: Oxford, 1974.

(2) Sinha, A.; Prasada Rao, T. A.; Dabrowski, R. Transient Electro-Optic Kerr Effect in Liquid Crystalline Isothiocyanates. *J. Phys. Soc. Jpn.* **1999**, *68*, 1939−1942.

(3) Carbone, G.; Barberi, R. Atomic Force Microscope Study of Presmectic Modulation in the Nematic and Isotropic Phases of the Liquid Crystal Octylcyanobiphenyl Using Piezoresistive Force Detection. *Phys. Rev. E* **2005**, *71*, 051704-1−051704-5.

(4) Krich, J. J.; Romanowsky, M. B.; Collings, P. J. Correlation Length and Chirality of the Fluctuations in the Isotropic Phase of Nematic and Cholesteric Liquid Crystals. *Phys. Rev. E* **2005**, *71*, 051712-1−051712-8.

(5) Hanson, E. G.; Shen, Y. R.; Wong, G. K. L. Optical-Field-Induced Refractive Indices and Orientational Relaxation Times in a Homologous Series of Isotropic Nematic Substances. *Phys. Rev. A* **1976**, *14*, 1281−1289.

(6) Stankus, J. J.; Torre, R.; Marshall, C. D.; Greenfield, S. R.; Sengupta, A.; Tokmakoff, A.; Fayer, M. D. Nanosecond Time Scale Dynamics of Pseudo-Nematic Domains in the Isotropic Phase of Liquid Crystals. *Chem. Phys. Lett.* **1992**, *194*, 213−216.

(7) Gierke, T. D.; Flygare, W. H. Depolarized Rayleigh Scattering in Liquids. Molecular Reorientation and Orientation Pair Correlations in a Nematic Liquid Crystal: MBBA. *J. Chem. Phys.* **1974**, *61*, 2231−2239.

(8) Stinson, T. W.; Litster, J. D. Correlation Range of Fluctuations of Short-Range Order in the Isotropic Phase of a Liquid Crystal. *Phys. Rev. Lett.* **1973**, *30*, 688−692.

(9) Litster, J. D. Critical Slowing of Fluctuations in a Nematic Liquid Crystal. *J. Appl. Phys.* **1970**, *41*, 996−997.

(10) Gottke, S. D.; Cang, H.; Bagchi, B.; Fayer, M. D. Comparison of the Ultrafast to Slow Time Scale Dynamics of Three Liquid Crystals in the Isotropic Phase. *J. Chem. Phys.* **2002**, *116*, 6339−6347.

(11) Cang, H.; Li, J.; Fayer, M. D. Short Time Dynamics in the Isotropic Phase of Liquid Crystals: The Aspect Ratio and the Power Law Decay. *Chem. Phys. Lett.* **2002**, *366*, 82−87.

(12) Moilanen, D. E.; Fenn, E. E.; Wong, D.; Fayer, M. D. Water Dynamics in Large and Small Reverse Micelles: From Two Ensembles to Collective Behavior. *J. Chem. Phys.* **2009**, *131*, 014704.

(13) Fenn, E. E.; Wong, D. B.; Fayer, M. D. Water Dynamics at Neutral and Ionic Interfaces. *Proc. Natl. Acad. Sci. U.S.A.* **2009**, *106*, 15243−15248.

(14) Zhu, X.; Farrer, R. A.; Fourkas, J. T. Ultrafast Orientational Dynamics of Nanoconfined Benzene. *J. Phys. Chem. B* **2005**, *109*, 12724−12730.

(15) Moilanen, D. E.; Piletic, I. R.; Fayer, M. D. Water Dynamics in Nafion Fuel Cell Membranes: The Effects of Confinement and Structural Changes on the Hydrogen Bonding Network. *J. Phys. Chem. C* **2007**, *111*, 8884−8891.

(16) Moilanen, D. E.; Fenn, E. E.; Wong, D.; Fayer, M. D. Water Dynamics in AOT Lamellar Structures and Reverse Micelles: Geometry and Length Scales Vs. Surface Interactions. *J. Am. Chem. Soc.* **2009**, *131*, 8318−8328.

(17) Sturlaugson, A. L.; Arima, A. Y.; Bailey, H. E.; Fayer, M. D. Orientational Dynamics in a Lyotropic Room Temperature Ionic Liquid. *J. Phys. Chem. B* **2013**, *117*, 14775−14784.

(18) Sturlaugson, A. L.; Fruchey, K. S.; Fayer, M. D. Orientational Dynamics of Room Temperature Ionic Liquid/Water Mixtures: Evidence for Water-Induced Structure and Anisotropic Cation Solvation. *J. Phys. Chem. B* **2012**, *116*, 1777−1787.

(19) Gray, G. W.; Harrison, K. J.; Nash, J. A. New Family of Nematic Liquid Crystals for Displays. *Electron. Lett.* **1973**, *9*, 130−131.

(20) Babkov, L. M.; Gnatyuk, I. I.; Puchkovskaya, G. A.; Trukhachev, S. V. Stucture and Conformational Mobility of 4′-Pentyl-4-Cyanobiphenyl from IR Spectroscopic Data. *J. Struct. Chem.* **2002**, *43*, 1019−1026.

(21) Sokolowsky, K. P.; Fayer, M. D. Dynamics in the Isotropic Phase of Nematogens Using 2D IR Vibrational Echo Measurements on Natural Abundance ^{13}CN and Extended Lifetime Probes. *J. Phys. Chem. B* **2013**, *117*, 15060−15071.

(22) Cang, H.; Li, J.; Novikov, V. N.; Fayer, M. D. Dynamics in Supercooled Liquids and in the Isotropic Phase of Liquid Crystals: A Comparison. *J. Chem. Phys.* **2003**, *118*, 9303−9311.

(23) Li, J.; Cang, H.; Anderson, H. C.; Fayer, M. D. A Mode Coupling Theory Description of the Short and Long Time Dynamics of Nematogens in the Isotropic Phase. *J. Chem. Phys.* **2006**, *124*, 014902.

(24) McMorrow, D.; Lotshaw, W. T.; Kenney-Wallace, G. A. Femtosecond Optical Kerr Studies on the Origin of the Nonlinear

Response in Simple Liquids. *IEEE J. Quantum Electron.* **1988**, *24*, 443−454.
(25) McMorrow, D.; Lotshaw, W. T. Intermolecular Dynamics in Acetonitrile Probed with Femtosecond Fourier Transform Raman Spectroscopy. *J. Chem. Phys.* **1991**, *95*, 10395−10406.
(26) Cang, H.; Li, J.; Novikov, V. N.; Fayer, M. D. Dynamical Signature of Two "Ideal Glass Transitions" in Nematic Liquid Crystals. *J. Chem. Phys.* **2003**, *119*, 10421−10427.
(27) Sjögren, L. Diffusion of Impurities in a Dense Fluid near the Glass Transition. *Phys. Rev. A* **1986**, *33*, 1254−1260.
(28) Cang, H.; Li, J.; Andersen, H. C.; Fayer, M. D. The Boson Peak in Supercooled Liquids: Time Domain Observations and Mode Coupling Theory. *J. Chem. Phys.* **2005**, *124*, 014902.
(29) Mukamel, S. *Principles of Nonlinear Optical Spectroscopy*; Oxford University Press: New York, 1995.
(30) Mukamel, S. Multidimensional Femtosecond Correlation Spectroscopies of Electronic and Vibrational Excitations. *Annu. Rev. Phys. Chem.* **2000**, *51*, 691−729.
(31) Park, S.; Kwak, K.; Fayer, M. D. Ultrafast 2D-IR Vibrational Echo Spectroscopy: A Probe of Molecular Dynamics. *Laser Phys. Lett.* **2007**, *4*, 704−718.
(32) Li, J.; Wang, I.; Fayer, M. D. Three Homeotropically Aligned Nematic Liquid Crystals: Comparixon of Ultrafast to Slow Time-Scale Dynamics. *J. Chem. Phys.* **2006**, *124*, 044906-1−044906-7.
(33) Ghanadzadeh, A.; Beevers, M. S. Dielectric Investigations and Molecular Association in Non-Mesogenic and Mesogenic Solutions. *J. Mol. Liq.* **2002**, *102*, 365−377.
(34) Smith, N. A.; Meech, S. R. Optically-Heterodyne-Detected Optical Kerr Effect (OHD-OKE): Applications in Condensed Phase Dynamics. *Int. Rev. Phys. Chem.* **2002**, *21*, 75−100.
(35) Kinoshita, S.; Sakai, Y.; Miyazaki, J.; Watanabe, J. Fundamental Aspects of Light Scattering and Optical Kerr Effect Spectroscopy. *Eur. Phys. J.: Spec. Top.* **2012**, *209*, 1−100.
(36) Nicolau, B. G.; Sturlaugson, A.; Fruchey, K.; Ribeiro, M. C. C.; Fayer, M. D. Room Temperature Ionic Liquid-Lithium Salt Mixtures: Optical Kerr Effect Dynamical Measurements. *J. Phys. Chem. B* **2010**, *114*, 8350−8356.
(37) Sturlaugson, A. L.; Fruchey, K. S.; Lynch, S. R.; Aragon, S. R.; Fayer, M. D. Orientational and Translational Dynamics of Polyether/Water Solutions. *J. Phys. Chem. B* **2010**, *114*, 5350−5358.
(38) Cang, H.; Novikov, V. N.; Fayer, M. D. Logarithmic Decay of the Orientational Correlation Function in Supercooled Liquids on the Ps to Ns Time Scale. *J. Chem. Phys.* **2003**, *118*, 2800−2807.
(39) Zheng, J.; Kwak, K.; Fayer, M. D. Ultrafast 2D IR Vibrational Echo Spectroscopy. *Acc. Chem. Res.* **2007**, *40*, 75−83.
(40) Kwak, K.; Park, S.; Finkelstein, I. J.; Fayer, M. D. Frequency-Frequency Correlation Functions and Apodization in 2D-IR Vibrational Echo Spectroscopy, a New Approach. *J. Chem. Phys.* **2007**, *127*, 124503.
(41) Kwak, K.; Rosenfeld, D. E.; Fayer, M. D. Taking Apart the Two-Dimensional Infrared Vibrational Echo Spectra: More Information and Elimination of Distortions. *J. Chem. Phys.* **2008**, *128*, 204505.
(42) Reddy, R. R.; Venkatesulu, A.; Rama Gopal, K.; Neelakanteswara Reddy, K. Thermo Acoustic Parameters in the Nematic and Isotropic Phases of 5CB and Tetraethyl Methane in 5CB. *J. Mol. Liq.* **2007**, *130*, 112−118.
(43) Oweimreen, G. A.; Shihab, A. K.; Halhouli, K.; Sikander, S. F. Density Measurements in the Nematic and Isotropic Phases of 5CB and Dilute Solutions of Tetraethylmethane in 5CB. *Mol. Cryst. Liq. Cryst.* **1986**, *138*, 327−338.
(44) Adamska, G.; Dabrowski, R.; Dziaduszek, J.; Kenig, K.; Zytynski, E. A Convenient Method for Obtaining Liquid Crystalline 4-N-Alkyl-4′-Cyanobiphenyls. *Biul. Wojsk. Akad. Tech. im. Jaroslawa Dabrowskiego* **1978**, *27*, 91−102.
(45) Dai, Z.; Zhang, W.; Zhang, Z.; Wei, B. Cross-Coupling Reaction of Grignard Reagents with Alkyl Halides Catalyzed by Green, Economical Copper Bromide Catalyst. *Adv. Mater. Res.* **2011**, *233*−*235*, 1119−1122.
(46) Akaike, H. New Look at Statistical-Model Identification. *IEEE Trans. Autom. Control* **1974**, *AC19*, 716−723.
(47) Götze, W.; Sperl, M. Nearly Logarithmic Decay of Correlations in Glass-Forming Liquids. *Phys. Rev. Lett.* **2004**, *92*, 105701.
(48) Götze, W.; Sjögren, L. The Mode Coupling Theory of Structural Relaxations. *Transp. Theory Stat. Phys.* **1995**, *24*, 801−853.
(49) Schweizer, K. S.; Chandler, D. Vibrational Dephasing and Frequency Shifts of Polyatomic Molecules in Solution. *J. Chem. Phys.* **1981**, *76*, 2296−2314.
(50) Bian, H.; Li, J.; Wen, X.; Zheng, J. Mode-Specific Intermolecular Vibrational Energy Transfer. I. Phenyl Selenocyanate and Deuterated Chloroform Mixture. *J. Chem. Phys.* **2010**, *132*, 184505-1−184505-8.